

Spin Fluctuation Dynamics and Multiband Superconductivity in Iron Pnictides

Valentin Stanev,¹ Jian Kang,¹ and Zlatko Tesanovic¹

¹*Department of Physics & Astronomy, The Johns Hopkins University, Baltimore, MD 21218*

(Dated: November 4, 2018)

Multiband superconductivity, involving resonant pair scattering between different bands, has emerged as a possible explanation of some of the main characteristics of the recently discovered iron pnictides. A key feature of such interband pairing mechanism is that it can generate or enhance superconducting pairing *irrespective* of whether it is attractive or repulsive. The latter case typically leads to the superconducting gap switching its sign among different sections of the Fermi surface. In iron pnictides, the natural scenario is that the gap changes sign between the hole and the electron Fermi surfaces. However, the macroscopic symmetry of such an extended s' -wave state still belongs to the general s -wave category, raising the question of how to distinguish it from an ordinary s -wave. In such a quest, it is essential to use experimental techniques that have a *momentum space* resolution and can probe momenta of order (π, π) , the wavevector that separates the hole and the electron Fermi surfaces in the Brillouin zone. Here we study experimental signatures in the spin fluctuation dynamics of the fully-gapped s - and s' -wave superconducting states, as well as those of the nodal d - and p -wave. The coupling between spin fluctuations of the incipient nearly-nested spin density-wave (SDW) and the Bogoliubov-deGennes quasiparticles of the superconducting state leads to the Landau-type damping of the former. The intrinsic structure of the superconducting gap leaves a distinctive signature in the form of this damping, allowing it to be used to diagnose the nature of iron-based superconductivity in neutron scattering and other experiments sensitive to spin fluctuations in momentum space. We also discuss the coexistence between superconductivity and SDW order.

INTRODUCTION

Recent discovery of a new high-temperature superconducting family [1, 2, 3, 4, 5, 6, 7, 8, 9] has generated a flurry of excitement. Many of the key questions, both theoretical and experimental, remain unanswered. However, it is becoming rapidly clear that the resemblance to the high- T_c cuprates is less straightforward and that a new superconducting mechanism might be at play.

Variety of order parameters and pairing mechanisms has been suggested. Phonon interaction alone seems too weak to explain high T_c . In several theoretical papers [10, 11, 12, 13] the multiband superconductivity is discussed as a possible explanation for the high T_c . Indeed, it has been long known [14] that multiband effects can strongly enhance superconductivity. This is a particularly relevant in the case of iron-pnictides, which appear to be moderately correlated electron systems, with large number of Fe d -bands at and near the Fermi level. Another advantage of this mechanism is that the interband pair interaction can enhance superconductivity *irrespective* of whether it is attractive or repulsive, provided that the gaps in different bands have the same or opposite signs, respectively. The former is the familiar s -wave while the latter is the extended s -wave superconductivity, or s' . This s' state, with the superconducting gap having the opposite sign on hole and electron sections of the Fermi surface (FS), emerges as a natural explanation for the superconductivity in Fe-based compounds, given the proximity of these materials to various nesting-driven spin density-wave (SDW) and related instabilities and absence of obvious strong attractive interaction.

The early point-contact Andreev reflection experiments indeed indicated a fully-gapped superconductor [15, 16] with no indication of cuprate-like nodes, consistent with this s' picture, provided that the hole and electron gaps are of a similar magnitude. The subsequent microwave [17] and ARPES [18, 19] experiments further fortified the case for s or s' state, also finding the fully-gapped superconductor with, in some instances, different gaps for the hole and the electron portions of the FS. In contrast, the NMR results are most naturally interpreted in terms of a d - or p -wave nodal state [20].

This state of affairs underscores the urgency of settling the issue of the gap structure by additional experimentation. Very recently, several papers [13, 21, 22, 23] elaborated different possible experimental signatures of the s' superconductivity as well as of some other forms of superconducting order, particularly in the NMR experiments. However, in view of the complexity of these materials and still relatively poor quality of the samples, it is unlikely that a single experiment is going to settle this issue unequivocally. More importantly, the s' state is in the same symmetry class as the standard s -wave and there is in principle no *macroscopic* experiment, analogous to the phase sensitive measurements in cuprates [24], which can distinguish the two in a decisive, qualitative fashion. Instead, the key difference between the s' - and the s -wave state is in the *momentum space*, not the real space, and thus one should concentrate on experiments that have the momentum space resolution and can probe the wavevectors around (π, π) , which separates the hole (Γ) and the electron (M) FS in the Brillouin zone.

To this end, and to further expand the range of the ex-

perimental techniques that can be used in this regard, in this paper we consider the spin fluctuations dynamics in the superconducting state of iron pnictides. We assume that the system is close to a nesting-driven spin density-wave (SDW) instability and compare different contributions to the damping of spin fluctuations arising from the Bogoliubov-deGennes (BdG) quasiparticle excitations in superconductors with s - and s' -wave gap. For completeness, we also consider the case with nodal p and d -wave symmetry of the gap function. This problem is the superconducting state analogue of the Landau damping in Fermi liquids. We find that the damping is qualitatively different in all of the above cases and thus can be used to diagnose the intrinsic, microscopic nature of the superconducting order. We also consider the situation in which the ordered SDW/AF state coexists with a superconductor. This coexistence is observed in at least two of the compounds [8, 9] and can be induced by pressure or doping.

PRELIMINARIES AND THE MODEL

The parent compound of the 1111 class of Fe-based superconductors has a ZrCuSiAs-type crystal structure [25], with eight atoms per unit cell. The Fe atoms lie in a plane, same as O atoms precisely above them, in the adjacent rare earth (RE) oxide layer. In contrast, the RE and As atoms (also located above each other) are puckered out of plane in a checkerboard fashion. This puckering of As atoms is crucial for understanding the electronic structure of the compounds [11]. It brings all Fe d -orbitals close to the Fermi level and creates significant overlap among Fe and As atomic orbitals. The result is a rich band structure. There are five bands crossing Fermi surface: two electron cylinders around M point; two hole cylinders plus a hole pocket around Γ point [10, 26, 27]. The 3D hole pocket is quickly filled with doping and is believed to be irrelevant to both antiferromagnetism and superconductivity. The remaining two hole and two electron bands are almost cylindrical and exhibit significant degree of nesting. The natural Fe magnetism, due to the Hund's rule, is suppressed and one is left with a weaker itinerant (antiferro)magnetism, sensitive to the nesting features in the band structure and associated with moderately strong correlations [11].

The outlines of the generic phase diagram of iron pnictides have begun to emerge [28, 29, 30]: at zero and moderate doping and zero temperature there is structural distortion and antiferromagnetic order which disappear at some higher temperature. This critical temperature is strongly suppressed by doping; at some critical doping structural distortion and antiferromagnetism suddenly give way to superconductivity. After this point, further increase in the doping level produces relatively small changes and the superconducting T_c is rather flat. In ad-

dition, $\text{SmO}_{1-x}\text{F}_x\text{FeAs}$ and $\text{Ba}_{1-x}\text{K}_x\text{Fe}_2\text{As}_2$ have a sizable region of coexistence of antiferromagnetism (SDW) and superconductivity.

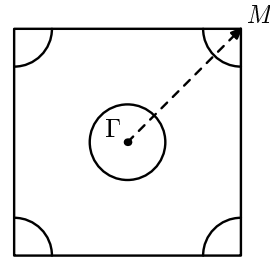


FIG. 1: An illustration of our model: a hole band (c) centered at the Γ point and an electron band (d) centered at the $M = (\pi, \pi)$ point interact via a short-range interaction U .

An emerging consensus is that antiferromagnetism is due to the nesting between the hole and the electron bands. The result is the spin density-wave (SDW) formed by itinerant electrons. After particle-hole transformation, the SDW instability is mathematically equivalent to the BCS one, caused by a logarithmic divergence [11]. Away from perfect nesting this divergence is replaced with a finite peak and sufficiently far away there is no instability for weak interactions. Because of proximity to such instability, however, there are enhanced spin fluctuations in the system. These fluctuations couple to the Fermi liquid quasiparticles and can decay into an electron-hole pair, which leads to a Landau-type damping. In the antiferromagnetically ordered state with localized spins or in a perfectly nested SDW one expects an insulating behavior. Instead, the experiments show a drop in the resistivity at the SDW transition point followed by the metallic behavior [31]. This obviously implies a high degree of itinerancy and indicates that the Fermi surface is only partially gapped or that the Fermi level is located entirely outside the SDW gap. In presence of the SDW order, the collective excitations of the SDW order parameter (spin waves) can interact with the quasiparticles on the Fermi surface, thus inducing a Landau-type damping of the former. Similarly, in the vicinity of the SDW state, when the true long range order is absent but the correlation length is very large, the spin fluctuations – the incipient spin-waves of the SDW – are also damped by the aforementioned decay into the particle-hole continuum. When the system undergoes the superconducting transition, this particle-hole continuum at the Fermi level is gapped by the superconducting order. Consequently, the new fermions – the BdG quasiparticles – are far less effective in damping the spin fluctuations and the decay rate vanishes as the temperature goes to zero. This decay rate of spin fluctuations carries a distinct signature of the structure of the superconducting gap in *momentum space* and the associated BCS coherence factors.

For the purposes of this paper we adopt the following simple yet sufficiently realistic model depicted in Fig. 1. We assume that the electron spectrum are described by two different bands: a hole (c) band at Γ point, and an electron (d) band at the $\vec{M} = (\pi, \pi)$ point with the same effective mass m . This is an approximation to be sure but a sensible one since the two hole and two electron bands at the FS of real Fe-pnictides resemble each other to a reasonable degree. In fact, Fe-pnictides are really *semimetals*, in the following sense: consider two bands

$$\begin{aligned}\epsilon_{\vec{p}}^c &= \epsilon_c + t_c \cos(p_x a) + t_c \cos(p_y a) \\ \epsilon_{\vec{p}}^d &= \epsilon_d + t_d \cos(p_x a) + t_d \cos(p_y a)\end{aligned}\quad (1)$$

and imagine the situation where $\epsilon_d - \epsilon_c \gg t_c, t_d$ and we have two electrons per unit cell, mimicking the six d electrons of the Fe-pnictides parent compounds. The chemical potential is in the gap between the c (full) and d (empty) bands and the system is an insulator. Now, as the difference $\epsilon_d - \epsilon_c$ is gradually reduced while the electron number remains unchanged, the bottom of the d band at the corner M of the Brillouin zone (BZ) moves below the top of the c band at its center Γ . The electrons filling the top of c now migrate to the bottom of d leaving the holes in c behind, thereby creating the FS shown in Fig. 1. The density of electrons filling the bottom of d is precisely equal to the density of holes in c band, hence the semimetal label for the parent compounds. Of course, the situation in real materials is not as simple as Eq. (1); there are four not two bands and they are far from being simple since their orbital content changes considerably as one goes around the FS [11]. These complexities notwithstanding, the above simple picture (Fig. 1 and Eq. (1)) with $t_c \sim t_d$ will suffice for the purposes of this paper.

The relevant interband interaction is assumed to be the short-ranged Hubbard U . Thus, the action and the Hamiltonian can be written as

$$\begin{aligned}S_0 &= \int d\tau d^d r \left\{ \bar{c}(\partial_\tau - \mu)c + \hat{H}^c + \bar{d}(\partial_\tau - \mu)d + \hat{H}^d \right\} \\ S_{int} &= U \int d\tau d^d r \bar{c} c \bar{d} d \\ \hat{H}^c &= \sum_{\vec{p}} \epsilon_{\vec{p}}^c \bar{c}_{\vec{p}} c_{\vec{p}} = \sum_{\vec{p}} \left(\epsilon_F - \frac{\vec{p}^2}{2m} \right) \bar{c}_{\vec{p}} c_{\vec{p}} \\ \hat{H}^d &= \sum_{\vec{p}} \epsilon_{\vec{p}}^d \bar{d}_{\vec{p}} d_{\vec{p}} = \sum_{\vec{p}} \left(-\epsilon_F + \frac{(\vec{p} - \vec{M})^2}{2m} \right) \bar{d}_{\vec{p}} d_{\vec{p}}\end{aligned}\quad (2)$$

where we have expanded c (d) band (1) near the top (bottom). We can now shift the electron band to the Γ point, and call this "new" electron band e . One should, however, always keep in mind that the two bands are shifted relative to each other in momentum space by $\vec{M} = (\pi, \pi)$ (Fig. 1).

First, we consider the case of perfect nesting $\mu = 0$ and compute the damping term for the spin fluctuations, given by the imaginary part of the electronic spin susceptibility:

$$\chi(\vec{q} + \vec{M}, \omega) = \sum_{\vec{p}} \frac{f(\epsilon_{\vec{p}+\vec{q}}^c) - f(\epsilon_{\vec{p}}^e)}{\omega - (\epsilon_{\vec{p}+\vec{q}}^c - \epsilon_{\vec{p}}^e) + i0^+}$$

which results in:

$$Im\chi(\vec{q} + \vec{M}, \omega) \propto \frac{\omega}{v_F q}, \quad (3)$$

having the familiar Landau damping form.

Next, we consider a more realistic case and assume that two bands are mismatched - their centers do not coincide - one being shifted by $\Delta\vec{k}_F$ - and furthermore their radii differ by 2μ , as illustrated in Fig. 2. These two quantities, $\Delta\vec{k}_F$ and μ , parameterize deviations from perfect nesting within our model. The spectrum of the two bands is:

$$\begin{aligned}\epsilon_{\vec{p}}^c &= \epsilon_F - \frac{\vec{p}^2}{2m} - \mu \\ \epsilon_{\vec{p}}^e &= -\epsilon_F + \frac{(\vec{p} + \Delta\vec{k}_F)^2}{2m} - \mu.\end{aligned}$$

Notice that the damping term is nonzero only if the two Fermi surfaces touch or intersect each other, otherwise it is impossible to excite an electron-hole pair with a low energy fluctuation and momentum close to \vec{M} . When two Fermi surfaces have two different intersection points, the damping term is proportional to ω :

$$\frac{\omega}{\sqrt{\left(\frac{P_0 |\Delta k_F|}{2m}\right)^2 - \mu^2}}, \quad (4)$$

where $P_0^2 = 2m\epsilon_F - (|\Delta k_F|/2)^2$.

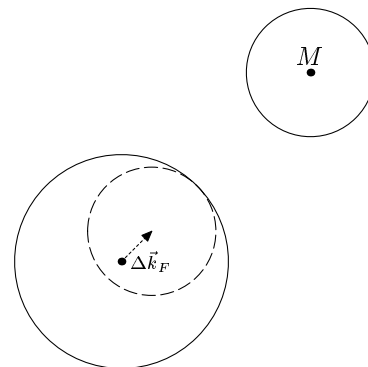


FIG. 2: Fermi surfaces of inequivalent hole and electron bands. Their centers are displaced by the vector $\Delta\vec{k}_F$ defined in the text.

When the two bands are touching each other at a point on the Fermi surface, $|\Delta k_F| = \sqrt{2m(\epsilon_F + \mu)}$ -

$\sqrt{2m(\epsilon_F - \mu)}$. For $\mu \ll \epsilon_F$ but still finite, the low frequency damping term is:

$$\text{Im}\chi(\vec{q} + \vec{M}, \omega) \propto \frac{\omega}{2\mu}. \quad (5)$$

SPIN FLUCTUATIONS IN A SUPERCONDUCTING STATE

Once our system enters the superconducting state, the damping changes and becomes temperature dependent reflecting the opening of the superconducting gap. The coupling of the spin fluctuations to the new excitations – the BdG quasiparticles – is determined by the BCS coherence factors [32]. These coherence factors, however, have a different form for different forms of the *microscopic* superconducting order parameter – the BdG gap function – and therein lies the possibility for diagnosing the intrinsic nature of the superconducting state.

Again, we first consider the case of perfect nesting between the hole and the electron band(s). Since we are interested in scattering of BdG quasiparticles and in the processes that involve spin, the correct coherence factor to use is $u_{\vec{p}}u_{\vec{p}+\vec{q}} + v_{\vec{p}}v_{\vec{p}+\vec{q}}$ or, explicitly:

$$\frac{1}{2} \left(1 + \frac{\epsilon_{\vec{p}}^c \epsilon_{\vec{p}+\vec{q}}^e + \Delta^c \Delta^e}{E_{\vec{p}}^c E_{\vec{p}+\vec{q}}^e} \right), \quad (6)$$

where $E_{\vec{p}}^c = \sqrt{(\epsilon_{\vec{p}}^c)^2 + (\Delta^c)^2}$ and $E_{\vec{p}}^e = \sqrt{(\epsilon_{\vec{p}}^e)^2 + (\Delta^e)^2}$. Since our focus is on spin fluctuations with momenta around $\vec{M} = (\pi, \pi)$, we are justified in dropping the intraband terms. The electron susceptibility then can be written as

$$\begin{aligned} \chi(\vec{q} + \vec{M}, \omega) &= \\ &= \sum_{\vec{p}} \frac{1}{2} \left(1 + \frac{\epsilon_{\vec{p}}^c \epsilon_{\vec{p}+\vec{q}}^e + \Delta_{\vec{p}}^c \Delta_{\vec{p}+\vec{q}}^e}{E_{\vec{p}}^c E_{\vec{p}+\vec{q}}^e} \right) \frac{f(E_{\vec{p}+\vec{q}}^c) - f(E_{\vec{p}}^e)}{\omega - (E_{\vec{p}+\vec{q}}^c - E_{\vec{p}}^e) + i0^+} \end{aligned} \quad (7)$$

where $q \ll M$. Extracting the imaginary part gives the general expression for damping of spin fluctuations at this momentum by the BdG particle-hole excitations:

$$\begin{aligned} \text{Im}\chi(\vec{M} + \vec{q}, \omega) &= \\ &= \sum_{\vec{p}} \frac{1}{2} \left(1 + \frac{\epsilon_{\vec{p}}^c \epsilon_{\vec{p}+\vec{q}}^e + \Delta_{\vec{p}}^c \Delta_{\vec{p}+\vec{q}}^e}{E_{\vec{p}}^c E_{\vec{p}+\vec{q}}^e} \right) \\ &\quad \times (f(E_{\vec{p}+\vec{q}}) - f(E_{\vec{p}})) \delta(\omega - (E_{\vec{p}+\vec{q}} - E_{\vec{p}})). \end{aligned} \quad (8)$$

First we consider the s' case. Because of $\Delta_{\vec{p}}^c = -\Delta_{\vec{p}+\vec{q}}^e$ (s' implies the repulsive pairing term) the coherence factor is strongly suppressed $E_{\vec{p}} E_{\vec{p}+\vec{q}} + \epsilon_{\vec{p}}^c \epsilon_{\vec{p}+\vec{q}}^e - \Delta_{\vec{p}} \Delta_{\vec{p}+\vec{q}} \approx \frac{1}{2}((v_F q \cos \theta)^2 (1 + (\frac{\epsilon_{\vec{p}}}{E_{\vec{p}}})^2))$, after expansion in the powers in q (we dropped the band indices for the moment and put $\epsilon_{\vec{p}}^c \equiv \epsilon_{\vec{p}}$). The argument of the δ -function in

(8) becomes (using $E_{\vec{p}+\vec{q}} - E_{\vec{p}} \approx \frac{\epsilon_{\vec{p}} v_F q \cos \theta}{E_{\vec{p}}}$ for small q) $\approx \omega - \frac{\epsilon_{\vec{p}} v_F q \cos \theta}{E_{\vec{p}}}$, with $\cos \theta$ having to be positive for $\epsilon_{\vec{p}}^c$. We can now use $\epsilon_{\vec{p}} = \sqrt{E_{\vec{p}}^2 - \Delta_{\vec{p}}^2}$ to solve for $E_{\vec{p}} \equiv E$:

$$\begin{aligned} \delta(\omega - (E_{\vec{p}+\vec{q}} - E_{\vec{p}})) &= \\ &= \frac{1}{v_F q \cos \theta} \frac{E^2 \sqrt{E^2 - \Delta^2}}{\Delta^2} \delta\left(E - \frac{\Delta}{\sqrt{1-x^2}}\right), \end{aligned}$$

where $x = \frac{\omega}{v_F q \cos \theta}$ is obviously smaller than unity; we will assume the condition $\frac{\omega}{v_F q} \ll 1$, as usual. The occupation number factor in Eq. (8), $f(E_{\vec{p}+\vec{q}}) - f(E_{\vec{p}})$, can be written as $f(E_{\vec{p}} + \omega) - f(E_{\vec{p}}) \approx \omega \frac{\partial f(E)}{\partial E}$. We then convert the p integration into E integration, with density of states $\frac{E}{\sqrt{E^2 - \Delta^2}}$, and perform the integral over the δ -function. This leaves us with only the angular integration remaining:

$$\begin{aligned} &\int_{-\frac{\pi}{2} - \frac{\omega}{v_F q}}^{\frac{\pi}{2} - \frac{\omega}{v_F q}} (v_F q \cos \theta) \left(-\frac{2E^2 - \Delta^2}{E \Delta^2} \right) \left(\omega \frac{\partial f(E)}{\partial E} \right) dE \\ &= \int_{-\frac{\pi}{2} - \frac{\omega}{v_F q}}^{\frac{\pi}{2} - \frac{\omega}{v_F q}} (v_F q \cos \theta) \frac{(1+x^2)}{\sqrt{1-x^2} \Delta} \omega \frac{\partial f(E)}{\partial E} dE, \end{aligned} \quad (9)$$

where $\frac{\partial f(E)}{\partial E}$ is evaluated at $E = \frac{\Delta}{\sqrt{1-x^2}}$. This integral is non-trivial and to perform it we have to use $\omega/v_F q \ll 1$. Despite the $\sqrt{1-x^2}$ in the denominator the integrand is rapidly suppressed in the limit $x \rightarrow 1$, because of the exponential factor hiding in $\frac{\partial f(E)}{\partial E}$. It is straightforward to check that the first derivative at $\theta = 0$ vanishes and that the integrand has a maximum there. Because of the rapid decrease away from this point, we can estimate the integral with the familiar formula $I \approx y(0) \sqrt{\frac{y(0)}{|y''(0)|}}$, where $y(\cos \theta)$ is the integrand. Working to the lowest order in $\frac{\omega}{v_F q}$ we finally obtain:

$$\text{Im}\chi^{s'}(\vec{q}, \omega) \propto \omega (v_F q) \frac{e^{\frac{\Delta}{T}}}{(e^{\frac{\Delta}{T}} + 1)^2 T}. \quad (10)$$

This expression gives the interband contribution to the damping of an incipient fluctuating spin wave in an s' -wave superconductor.

It is instructive to contrast the above result with the standard s -wave case. After performing the analogous calculation for the case of a pure s -wave superconductor, the coherence factor for the superconductor is found to have a constant term $\sim \frac{\Delta^2}{E^2}$. Keeping only this term and going through the same steps as before yields:

$$\text{Im}\chi^s(\vec{q}, \omega) \propto \frac{\omega}{v_F q} \frac{e^{\frac{\Delta}{T}}}{(e^{\frac{\Delta}{T}} + 1)^2 T}. \quad (11)$$

Clearly, the dynamical properties of spin fluctuations in s and s' superconducting phase are very different: the

damping and thus the decay rate of incipient spin waves in the s' state is substantially reduced relative to the standard s -wave case, by the overall factor of q^2 (note that \vec{q} is measured *relative* to \vec{M}). These differences and the specific forms of damping should be observable in neutron scattering or other momentum-resolved probes of spin fluctuations.

For completeness, we now consider the nodal d - and p -wave superconductors, another possible contenders for the superconducting state of iron pnictides, favored by the NMR experiments [20]. In this case, the main contribution to the low temperature damping comes from the nodal regions. The natural excitations of the system in this regions are Dirac fermions with linear dispersion $v_F|p|$, which can be seen by expanding the BdG Hamiltonian near the nodes [33]. We will ignore the intrinsic anisotropy of the BdG-Dirac spectrum, since we do not expect it is to change the overall form of the damping term. The coherence factors for the individual nodes differ for the intra and interband processes, but we need to add all the nodal contributions. The combined coherence factors are equal to lowest order (up to a numerical prefactor). First, we assume the $p_x p_y$ d -wave order parameter (d_{xy}), which means that the direction of \vec{M} and the nodal directions are rotated by $n\pi/4$ (where n is integer) with respect to each other. We expand around that nodes and do the momentum integral first, using the δ -function:

$$\omega \int \delta(\omega - E_{p+q} + E_p) \frac{\partial f(\epsilon)}{\partial \epsilon} E dE,$$

where now $E = v_F \sqrt{p_x^2 + p_y^2}$ is the linear dispersion of the Dirac quasiparticles. The integrand in the remaining angular integral is confined in the region $\theta \in (\pi/2, 3\pi/2)$, and is peaked around $\theta = \pi$. We again use the formula $I \approx y(0) \sqrt{\frac{y(0)}{|y''(0)|}}$ to estimate the lowest order contribution. This gives the final low temperature limit result:

$$\text{Im}\chi^{d_{xy}}(\vec{q}, \omega) \propto \omega \sqrt{q_x^2 + q_y^2} \frac{1}{T \cosh^2 \frac{|q|}{T}}. \quad (12)$$

The reason for this particular temperature dependence is the fact that we have restricted ourselves to the region $\omega \ll v_F q$. Integrating this expression over q we can obtain the standard result for the NMR damping rate $1/(T_1 T) \propto T^2$.

The other possibility for a d -wave order parameter is a $d_{x^2-y^2}$. In this case the nodal directions are along \vec{M} or perpendicular to it. To the lowest order the damping in this case has the same form as in the d_{xy} case, so the position of the nodes with respect to \vec{M} is irrelevant. We emphasize that this is only the lowest order result, so in general some distinction between the d_{xy} and $d_{x^2-y^2}$ cases is expected.

Now let us consider a p -wave superconductor with two nodes along x direction. Combining the coherence factors for the nodes gives an additional factor of $\sin^2 \theta$, compared to the d_{xy} case. We again use the δ -function to do the momentum integral first. After that the integrand is confined in the $(\pi/2, 3\pi/2)$ interval, but now goes to zero at $\theta = \pi$. Nonetheless, we can still estimate the integral and the leading term behavior is the same as in the d_{xy} case (with a different numerical prefactor):

$$\text{Im}\chi^{p_x}(\vec{q}, \omega) \propto \omega \sqrt{q_x^2 + q_y^2} \frac{1}{T \cosh^2 \frac{|q|}{T}}. \quad (13)$$

We obtain the same result for a p -wave superconductor with nodes along the \vec{M} direction.

A multigap nodal superconductor can also be an extended d and p -wave, with sign change between the gaps on the disconnected parts of the Fermi surface: a d' or p' state. The lowest order term in the coherence factor is then proportional to q^2 , as in the case of s' superconductor, and the damping in d' and p' states is strongly suppressed compared to the pure d and p -waves. We see that momentum resolved measurements can distinguish the p and d -wave superconductor from the s and s' case. This comes in addition to the significant differences in their temperature behavior.

Perfectly nested bands generate strong spin and charge density-wave (SDW and CDW) instabilities. It is believed that superconductivity appears with doping or by application of pressure, away from the perfect nesting, once the ordering in the particle-hole channel is suppressed. Thus, we now turn to the case of imperfect nesting. To this end, we again consider the two bands – a hole and an electron one, illustrated in Fig. 2. We also assume that the deviation from perfect nesting is small and Δk_F is of the order of q and smaller than Δ/v_F . Now expanding the coherence factor in the s' case gives us $\frac{1}{2}(2\mu + \vec{p} \cdot (\vec{q} + \Delta \vec{k}_F)/m)^2 (1 + (\frac{\epsilon}{E_p})^2)$. Repeating the same steps as before we obtain the damping:

$$\begin{aligned} \text{Im}\chi^{s'}(\vec{q}, \omega) &\propto \omega (2\mu + v_F |\vec{q} + \Delta \vec{k}_F|) \times \\ &\times \sqrt{\frac{2\mu + v_F |\vec{q} + \Delta \vec{k}_F|}{v_F |\vec{q} + \Delta \vec{k}_F|}} \frac{e^{\frac{\hbar}{T}}}{(e^{\frac{\hbar}{T}} + 1)^2 T}. \end{aligned} \quad (14)$$

For the s -wave superconductor coherence factor we again keep only Δ^2 term and the result is

$$\begin{aligned} \text{Im}\chi^s(\vec{q}, \omega) &\propto \frac{\omega}{2\mu + v_F |\vec{q} + \Delta \vec{k}_F|} \times \\ &\times \sqrt{\frac{2\mu + v_F |\vec{q} + \Delta \vec{k}_F|}{v_F |\vec{q} + \Delta \vec{k}_F|}} \frac{e^{\frac{\hbar}{T}}}{(e^{\frac{\hbar}{T}} + 1)^2 T}. \end{aligned} \quad (15)$$

Both results reduce correctly to the perfect nesting case ($\mu \rightarrow 0, \Delta k_F \rightarrow 0$) but generally have more complicated behavior. Increasing the mismatch of the two

bands drives the damping to the same form $const \times \omega$ in both cases, albeit with different constants.

In the case of d - and p -wave superconductors, the imperfect nesting of this type leads to a rather complicated behavior. The point where the two Fermi surfaces touch (Fig. 2) is special and its position with respect to the nodes determines the low-energy, low-temperature response. If there is a node in a close vicinity of this point of contact between two Fermi surfaces, the behavior of the system is somewhat similar to a perfectly nested single node case, but with \vec{M} replaced by $\vec{M} + \Delta\vec{k}_F$. If this point is in one of the anti-nodal regions the response resembles the one found in the s -wave case.

We pause here to emphasize again that the expressions for damping of spin fluctuations presented above – and similar other physical quantities – at a *specific* momentum around \vec{M} are better suited to distinguish between different *microscopic* order parameters and their associate BdG gap functions. In contrast, the NMR relaxation rate is an integral quantity and thus always includes *both* the interband *and* the intraband contributions. Extracting one of them is thus a rather challenging task. For example, even in the s' case, the Hebel-Slichter peak is expected to occur [23], due to the intraband (pure s) processes.

COEXISTENCE OF SUPERCONDUCTIVITY AND SDW

We now consider the combination of SDW and superconducting orders. We will assume that the main SDW (particle-hole) gap opens below the Fermi level, so the system remains metallic, as it appears to be the case experimentally [31]. This is depicted in Fig. 3 and it emulates the situation in real Fe-pnictides, where the mismatch among hole and electron pockets results in reconstruction instead of complete disappearance of the Fermi surface [11, 34]. Then – on top of this SDW – either attractive or sufficiently strongly repulsive interband interaction generates at some lower temperature a new *superconducting* (particle-particle) gap, this time located precisely on the Fermi surface (see Fig. 3). The question is whether spin waves dynamics can be used as a probe of the *microscopic* structure of the superconducting order parameter in this case as well.

The magnon (spin-wave) dispersion relation is given by the inverse of the transverse magnetic susceptibility χ^{+-} and is $\omega^2 - c^2q^2$ at the bare level, where c is the spin-wave velocity. Damping will be introduced by including magnon-electron interactions, as before. Here we neglect contributions from impurities and higher order magnon-magnon interactions; these are generally present but can be distinguished from the itinerant particle-hole damping by their different and lesser sensitivity to the opening of the superconducting gap. Then the imaginary part of

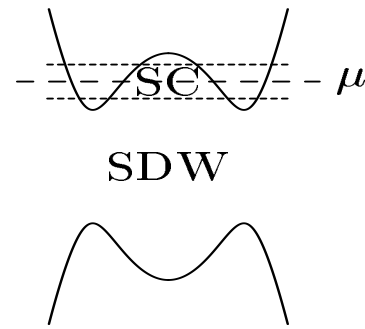


FIG. 3: Coexistence of spin density wave (SDW) and superconductivity in our model. The chemical potential μ is above the SDW gap while the superconducting gap is always pinned to μ .

the electron spin susceptibility χ determines the decay rate of magnons. In the SDW-only phase we have to rewrite the electron operators as a superposition of the new eigenstates, which diagonalize the broken symmetry Hamiltonian. This leads to the appearance of new coherence factors, reflecting the SDW order in the particle-hole channel [35]. Since we are interested in scattering of quasiparticles and in processes that involve spin, the correct coherence factor to use is $u_{\vec{p}}u_{\vec{p}+\vec{q}} - v_{\vec{p}}v_{\vec{p}+\vec{q}}$:

$$\frac{1}{2} \left(1 - \frac{\epsilon_{\vec{p}}\epsilon_{\vec{p}+\vec{q}} + \phi_0^2}{\xi_{\vec{p}}\xi_{\vec{p}+\vec{q}}} \right) \quad (16)$$

where $\epsilon_{\vec{p}} = p^2/2m - \epsilon_F$ and $\xi_{\vec{p}} = \sqrt{\epsilon_{\vec{p}}^2 + \phi_0^2}$, with ϕ_0 being the SDW order parameter.

In presence of the SDW, the unit cell doubles and \vec{M} becomes a vector of the reciprocal lattice. We can picture the new band structure with two bands at the same position in momentum space, with avoided crossing where the SDW gap opens. What was previously a hole-like (electron-like) band now has an electron-like (hole-like) part as well.

One important point should be discussed here. To have metallic behavior and superconductivity on the top of SDW we have to introduce the non-zero chemical potential for the new (gapped) band structure. This, however, cannot be done cavalierly, since the model will not be self-consistent. That is the consequence of the fact that within the simple model adopted in this paper, a gap on the Fermi surface is typically energetically preferable to a gap below or above. To remedy this and stabilize the SDW gap below the Fermi surface, we have to include new terms in our Hamiltonian, reflecting deviations from idealized bands and the lattice effects in real iron pnictides. This, unfortunately, comes at the cost of significantly more complicated calculations and an entirely obscured physical picture. For the purposes of this paper, this is too great a cost and we avoid it by using the following approach: we calculate the SDW

wave coherence factors at zero chemical potential, when Fermi surface is completely gapped. Next, in order to account for the metallic behavior, we reintroduce a small Fermi surface, which now can undergo a superconducting instability. The physics behind this approach is clear: the SDW coherence factors determine the vertices that couple the magnons and the BdG quasiparticles. The magnons are the Goldstone modes of the SDW and this coupling should be of a gradient type, because of the broken symmetry of the ordered state – the long wavelength twist in the spin direction of the SDW should come at no cost in energy. This remains true independently of the position of the SDW gap. Adopting this simplification, the SDW coherence factor is just $\sim (v_F q \cos \theta)^2$.

Starting with the case without superconductivity, the damping is:

$$\text{Im}\chi(\vec{q}, \omega) \propto \frac{\omega^3}{v_F q} \frac{\mu \phi_0^2}{4(\mu^2 - \phi_0^2)^2}. \quad (17)$$

In the case of coexistence we have to calculate anew the *superconducting* coherence factor

$$\frac{1}{2} \left(1 + \frac{\xi_{\bar{p}} \xi_{\bar{p}+\vec{q}} + \Delta_{\bar{p}} \Delta_{\bar{p}+\vec{q}}}{E_{\bar{p}} E_{\bar{p}+\vec{q}}} \right). \quad (18)$$

In the vicinity of the SDW gap, the new quasiparticles are almost an equal mixture of the two initial bands, *c* and *d*. Turning on the chemical potential moves the Fermi level to the upper band; as discussed above this is to be done advisedly. If the chemical potential is not very small, the content of the quasiparticles at the new Fermi level will be almost exclusively from only one of the old bands (either purely an electron-like or a hole-like). With this assumption we calculate the superconducting coherence factors.

Again, we first consider the *s'* case. Working to lowest order in ω/q we get:

$$\text{Im}\chi(\vec{q}, \omega) \approx \omega (v_F q)^3 \frac{e^{\frac{\Delta}{T}}}{(e^{\frac{\Delta}{T}} + 1)^2 T}. \quad (19)$$

This expression gives the interband contribution to the spin wave damping in an *s'*-wave superconductor. However, here we cannot neglect the intraband contribution as we did earlier, since now the momenta \vec{M} and 0 are effectively equivalent by virtue of the umklapp scattering off the underlying SDW modulation – consequently *both* inter and intraband terms are contributing. Calculating the intraband term gives:

$$\text{Im}\chi(\vec{q}, \omega) \approx \omega (v_F q) \frac{e^{\frac{\Delta}{T}}}{(e^{\frac{\Delta}{T}} + 1)^2 T}. \quad (20)$$

and we see that this is in fact the leading term in the limit $q \rightarrow 0$, masking the contribution of the interband damping.

For the case of a pure *s*-wave superconductor we get

$$\text{Im}\chi(\vec{q}, \omega) \approx \omega (v_F q) \frac{e^{\frac{\Delta}{T}}}{(e^{\frac{\Delta}{T}} + 1)^2 T}. \quad (21)$$

The intraband term is of the same order.

	pure SDW	<i>s'</i> SC	<i>s</i>	$d_{x^2-y^2}$	p_x
perfect nesting	$\frac{\omega^3}{q}$	$\omega q e^{-\frac{\Delta}{T}}$	$\frac{\omega}{q} e^{-\frac{\Delta}{T}}$	$\frac{\omega q }{T \cosh^2 \frac{ q }{T}}$	$\frac{\omega q }{T \cosh^2 \frac{ q }{T}}$
imperfect nesting	ω	$(2\mu + \alpha_{\vec{q}}) e^{-\frac{\Delta}{T}} \times$ $\times \omega \sqrt{\frac{2\mu + \alpha_{\vec{q}}}{\alpha_{\vec{q}}}}$	$\frac{\omega}{(2\mu + \alpha_{\vec{q}})} e^{-\frac{\Delta}{T}} \times$ $\times \sqrt{\frac{2\mu + \alpha_{\vec{q}}}{\alpha_{\vec{q}}}}$		

TABLE I: The summary of our results for damping of spin fluctuations by particle-hole excitations in several different superconducting states. Here $\alpha_{\vec{q}} = v_F |\vec{q} + \Delta \vec{k}_F|$.

Thus, in the region of coexistence, the dynamical properties of SDW magnons in an *s* and *s'* superconductor are difficult to distinguish. The damping at momentum around \vec{M} is due to both inter and intraband scattering and since the latter are, of course, unaffected by the relative sign of the different gaps, it would be difficult to observe any significant difference in experiments.

Table I summarizes some of our results for the reader's convenience.

A SIMPLE MODEL OF MULTIBAND SUPERCONDUCTIVITY

A significant part of our focus in this paper was on an *s'*-wave superconductor, in which the Fermi surface of Fig. 1 is fully gapped but the gap function in its hole pocket has the opposite sign relative to the one in the electron pocket. Furthermore, our paper is clearly designed to arouse interest in the experimental community. Consequently, for the reader's benefit, we consider here a rather basic picture of *s'* multiband superconductivity and some of its features, appropriate for our simplified model of Fe-pnictides (for a more theoretically inclined discussion, the reader is referred to [34]). With appropriate modifications, the same considerations can be easily adapted to the *d'* and *p'* cases.

First, the model (2) discussed so far is not sufficient. The interband interaction $U\bar{c}\bar{d}\bar{d}$ will induce the SDW and promote strong spin fluctuations but will not by itself lead to superconductivity from purely electronic interactions [34]. For that possibility to enter into play, one must consider the interband pair resonance interactions of the type $J\bar{c}\bar{d}\bar{d} + h.c.$, a Josephson-like term in the momentum space which scatters pairs of electrons between *c* and *d* bands [13, 34]. Such terms are typically present in multiband systems and their size in Fe-pnictides is significant [34].

The key feature of this interband interaction J is that it can drive the system superconducting – or enhance the already present intraband superconductivity – *irrespective* of whether it is attractive or repulsive. In the former case, the intraband gaps will have the same relative sign while in the latter, which is probably where the Fe-pnictides belong, this sign will be different. This is the origin of the s' superconducting state.

In the weak-coupling theory, however, the interband repulsive interaction J can drive the system superconducting *only* if it is large enough, i.e., $J^2 > U_1 U_2$, where U_1 and U_2 are the *repulsive* intraband interactions in the hole (c) and electron (d) bands. Such a sizeable J is not something that is easily found, since, generically, J is significantly smaller than the intraband Coulomb repulsion U_1, U_2 ; indeed, this also appears to be the case in Fe-pnictides [34]. Here we suggest a mechanism that could potentially solve this problem. The interactions that enter the condition for superconductivity are not the bare Coulomb terms but some appropriately screened interactions. The screening length is $\kappa_D = 4\pi e^2 \Pi_0(q)$, where $\Pi_0(q)$ is a polarization bubble. The momentum region for the J pairing term is around M and the main contribution to the polarization is a mixed bubble. On the other hand the main region for the $U_{1,2}$ terms is around 0 and the screening is due mostly to the usual single-band bubbles. $\kappa_D(\vec{M})$ has a rather dramatic evolution with doping [11] (in contrast with $\kappa_D(0)$), and goes to 0 for high doping levels. Let's now confine ourselves to the region in which the interactions are frequency independent. This limit is constrained by the time τ it takes an electron to traverse the Debye screening length $\tau \approx \frac{r_D}{v_F}$ where $r_D = \frac{1}{\kappa_D} = \frac{1}{4\pi e^2 \Pi_0}$. The interaction is frequency independent for $\omega \ll \frac{1}{\tau}$. Outside this region it has complicated frequency dependence and we can set $J = 0$ (as it is done in the extensions of the BCS theory which include Coulomb interaction, where $J = \text{const}$ for $\omega < \omega_C$ and $J = 0$ for $\omega > \omega_C$, where ω_C is the Coulomb frequency cut-off). For $\kappa_D(0) > \kappa_D(\vec{M})$, the frequency range of J is *smaller* and this could lead to logarithmic suppression of $U_{1,2}$ akin to the reduction in the Coulomb pseudopotential caused by phonon retardation effects within the standard BCS-Eliashberg theory [36].

We now illustrate the above arguments with an explicit calculation. In multiband superconductivity there are at least two gaps which vanish at the same critical temperature (if there is a non-vanishing pair resonance term J). We can write down the equations determining the zero temperature gaps and the critical temperature [14, 37]. To study the effects of the retardation we divide the energy range into two intervals: $\epsilon \in (0, \omega_{C1})$ and $\epsilon \in (\omega_{C1}, \omega_{C2})$, where ω_{C1} and ω_{C2} are the frequency cut-offs for J and $U_{1,2}$ respectively. For each band we define two gaps, Δ_{i1} and Δ_{i2} ($i = 1, 2$ is the band index), corresponding to these two regions. Assuming parabolic

bands as before, the gap equations are:

$$\begin{aligned} \Delta_{11} &= -\Delta_{11}\mu_1 \int_0^{\omega_{C1}} \frac{\tanh(\beta E_{11}/2)}{E_{11}} d\epsilon + \\ &\quad -\Delta_{21}\lambda_2 \int_0^{\omega_{C1}} \frac{\tanh(\beta E_{21}/2)}{E_{21}} d\epsilon - \\ &\quad -\Delta_{12}\mu_1 \int_{\omega_{C1}}^{\omega_{C2}} \frac{\tanh(\beta E_{12}/2)}{E_{12}} d\epsilon \\ \Delta_{12} &= -\Delta_{11}\mu_1 \int_0^{\omega_{C1}} \frac{\tanh(\beta E_{11}/2)}{E_{11}} d\epsilon - \\ &\quad -\Delta_{12}\mu_1 \int_{\omega_{C1}}^{\omega_{C2}} \frac{\tanh(\beta E_{12}/2)}{E_{12}} d\epsilon \end{aligned} \quad (22)$$

where $E_{ki} = \sqrt{\epsilon_{ki}^2 + \Delta_{ki}^2}$. To simplify the notation we have introduced new variables $\mu_{1,2} = N_{1,2}U_{1,2}$ and $\lambda_{1,2} = N_{1,2}J$, where N_i is the density-of-states (DOS) in band i . Both μ_i and λ_i are positive corresponding to repulsive interactions. The above equations are coupled with the analogous ones for Δ_{21} and Δ_{22} . The interactions J, U_1 , and U_2 appearing here are the angular averages over the Fermi surface [34].

To proceed, we concentrate on the condition for a non-trivial solution in terms of Δ_{ki} . This gives an equation for the integrals I_1 and I_2 that appear in Eq. (22):

$$\begin{aligned} I_1 &= \int_0^{\omega_{C1}} \frac{\tanh(\beta E_{11}/2)}{E_{11}} d\epsilon \\ I_2 &= \int_{\omega_{C1}}^{\omega_{C2}} \frac{\tanh(\beta E_{12}/2)}{E_{12}} d\epsilon. \end{aligned} \quad (23)$$

These integrals are positive-definite and close to the critical temperature can be approximated by $I_1 = \log(1.13\omega_{C1}/T_c)$ and $I_2 = \log(\omega_{C2}/\omega_{C1})$. If we now momentarily suspended the above "retardation" effect of J relative to $U_{1,2}$ ($\omega_{C2} = \omega_{C1}$) and take the cut-off of the energy integration to be the same everywhere $I_2 \rightarrow 0$ and I_1 becomes

$$I_1 = \frac{(\mu_1 + \mu_2) + \sqrt{(\mu_1 - \mu_2)^2 + 4\lambda_1\lambda_2}}{2(\lambda_1\lambda_2 - \mu_1\mu_2)}. \quad (24)$$

The physical solution exists *only* if the right-hand side is positive, which translates into $\lambda_1\lambda_2 > \mu_1\mu_2$. Solving for the critical temperature we get:

$$T_c = (1.13\omega_C) e^{-\frac{(\mu_1 + \mu_2) + \sqrt{(\mu_1 - \mu_2)^2 + 4\lambda_1\lambda_2}}{2(\lambda_1\lambda_2 - \mu_1\mu_2)}}. \quad (25)$$

The full expression for T_c , obtained from Eq. (22), with $\omega_{C2} > \omega_{C1}$ and under the same conditions $I_1 > 0$ and $I_2 > 0$, is more complicated

$$T_c = (1.13\omega_{C1}) \times e^{-\frac{(\mu_1 + \mu_2 + 2I_2\mu_1\mu_2) + \sqrt{(\mu_1 - \mu_2)^2 + 4\lambda_1\lambda_2(1 + I_2\mu_1)^2(1 + I_2\mu_2)^2}}{2(\lambda_1\lambda_2(1 + I_2\mu_1)(1 + I_2\mu_2) - \mu_1\mu_2)}}. \quad (26)$$

As it turns out, however, once the retardation effect *is* restored, all the reader needs to do to obtain a good approximation to (26) is to simply replace in (25) $\mu_{1,2} \rightarrow \mu_{1,2}^*$, where $\mu_{1,2}^*$ are given by:

$$\mu_{1,2}^* = \frac{\mu_{1,2}}{1 + \mu_{1,2} \log(\omega_{C2}/\omega_{C1})}. \quad (27)$$

Therefore, now $\lambda_1 \lambda_2$ only has to be larger than $\mu_1^* \mu_2^*$, or, in the original notation $J > \sqrt{U_1^* U_2^*}$, to make s' superconductivity possible. Notice that, in a similar vein, any reduction in $U_{1,2}$ arising from the interband phonon attraction would help superconductivity as well.

One of the consequences of Eqs. (22) is that the overall magnitudes of the hole and electron gaps, $|\Delta_1|$ and $|\Delta_2|$, are generically different, as soon as the c and d band parameters are not the same. Several point-contact Andreev reflection (PCAR) measurements [15, 16], however, show a single gap. Obviously, one explanation is that there are two gaps, but they have similar magnitudes in this particular system and cannot be resolved in a PCAR experiment.

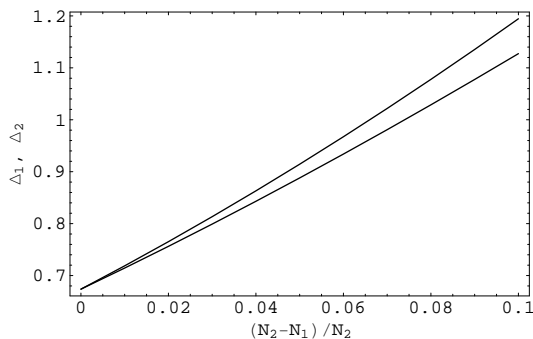


FIG. 4: The illustration of the relatively mild sensitivity of the two superconducting gaps to differences in the DOSs between electron and hole bands $((N_2 - N_1)/N_2)$. The gaps were computed from Eq. (22), without retardation effects, using $\mu_1 = 0.3$ and $\lambda_1 = 0.5$, for up to 10% difference in DOSs, and are measured in units of $10^{-2}\omega_C$.

In contrast, the ARPES experiments do in fact show two different gaps in some of the other Fe-pnictide superconductors [18, 19]. Note that the main role of different band parameters arises through their different densities-of-states (DOSs), the parameter which is independent of doping for 2D parabolic bands. Naturally, the real hole and electron bands in Fe-pnictides are neither ideal parabolas nor identical to each other (nor entirely 2D for that matter). To study the effects of different DOSs for the two bands we solve numerically Eq. (22) (without the retardation effects) at zero temperature for differences in DOS of the two bands of up to 10%. The result is shown in Fig 4 and we see that the hole and electron gaps diverge away from one another rather slowly. This illustrates the relative lack of sensitivity of the gap functions to differences in the band parameters, retroactively

provides another justification for our assuming that they are the same, and, within the framework of the s' -wave state, can explain the experiments that seemingly point to a single-gap superconductivity.

DISCUSSION AND CONCLUSIONS

In this paper we investigated the dynamical properties of spin fluctuations in superconductors with various forms of the microscopic order parameter, both in the vicinity of and within the itinerant SDW state. Our main emphasis was on finding ways to distinguish different types of superconducting order by concentrating on the features in *momentum* space, since one of the leading candidates, the extended s' -wave superconductor, does not differ from an ordinary s -wave by the overall symmetry. We demonstrated by explicit calculations that the momentum as well as the frequency dependence of the spin fluctuation decay rate can be used to distinguish among different states of a multiband, multigap superconducting system, even in the cases when the temperature dependence is similar; some of our results are summarized in Table I. Among other applications, we expect our findings to be particularly useful in the ongoing efforts to establish the symmetry of the order parameter in the iron-based high-temperature superconductors.

ACKNOWLEDGEMENTS

We thank V. Cvetkovic, C. Broholm and W. Bao for useful discussions. This work was supported in part by the NSF grant DMR-0531159.

-
- [1] Y. Kamihara, *et al.*, J. Am. Chem. Soc. **130**, 3296 (2008).
 - [2] X. H. Chen, *et al.*, Nature **453**, 761 (2008).
 - [3] G. F. Chen, *et al.*, Phys. Rev. Lett. **100**, 247002 (2008)
 - [4] Z.-A. Ren, *et al.*, Europhys. Lett. **82**, 17002 (2008).
 - [5] H. H. Wen, *et al.*, Europhys. Lett. **82**, 17009 (2008).
 - [6] M. Rotter, *et al.*, cond-mat/0805.4130.
 - [7] G. F. Chen, *et al.*, cond-mat/0806.1209.
 - [8] A. J. Drew, *et al.*, cond-mat/0806.
 - [9] H. Chen, *et al.*, cond-mat/0807.3950.
 - [10] I. I. Mazin, *et al.*, cond-mat/0803.2740.
 - [11] V. Cvetkovic and Z. Tesanovic, cond-mat/0804.4678.
 - [12] F. Wang, *et al.*, cond-mat/0807.0498.
 - [13] A. V. Chubukov, *et al.*, cond-mat/0807.3735.
 - [14] H. Suhl, B. T. Matthias, and L. R. Walker, Phys. Rev. Lett. **3**, 522 (1959).
 - [15] T. Y. Chen, Z. Tesanovic, R. H. Liu, X. H. Chen, and C. L. Chien, Nature **453**, 1224 (2008).
 - [16] P. Samuely, *et al.*, cond-mat/0806.1672.
 - [17] K. Hashimoto, *et al.*, cond-mat/0806.3149.
 - [18] H. Ding, *et al.*, cond-mat/0807.0419.
 - [19] L. Wray, *et al.*, cond-mat/0808.2185.

- [20] K. Matano, *et al.*, cond-mat/0806.0249.
- [21] T. A. Maier, *et al.*, cond-mat/0805.0316.
- [22] D. Parker, *et al.*, cond-mat/0807.3729.
- [23] M. M. Parish, *et al.*, cond-mat/0807.3950.
- [24] C.C. Tsuei and J.R. Kirtley, *Rev. Mod. Phys.* **72**, 969 (2000).
- [25] P. Quebe, L. J. Terbüchte, and W. Jeitschko, *J. Alloy. Compd.* **302**, 70 (2000).
- [26] F. Ma, Z.-Y. Lu, T. Xiang, cond-mat/0804.3370.
- [27] S. Lebègue, *Phys. Rev. B* **75**, 035110 (2007).
- [28] C. de la Cruz, *et al.*, *Nature* **453**, 899 (2008).
- [29] S. Margadonna, *et al.*, cond-mat/0806.3962.
- [30] H. Chen, *et al.*, cond-mat/0807.3950; Y. Qiu, *et al.*, cond-mat/0806.2195.
- [31] D. Bhoi, P. Mandal, and P. Choudhury, arXiv:0807.3833.
- [32] M. Tinkham, *Introduction to Superconductivity*, McGraw-Hill, New York, 1996.
- [33] S. H. Simon and P. A. Lee, *Phys. Rev. Lett* **78**, 1548 (1997).
- [34] V. Cvetkovic and Z. Tesanovic, cond-mat/0808.3742.
- [35] M. Gruner, *Density waves in solids*, Addison-Wesley, 1994.
- [36] The reader should be warned that these arguments are an oversimplification. In real materials, the reliable computations of such dynamical screening are far more demanding and involve the so-called local-field corrections to the dielectric function; see P. B. Littlewood, *Phys. Rev. B* **42**, 10075 (1990) and references therein.
- [37] J. Kondo, *Prog. Teor. Phys* **29**, 1 (1963).